Tropical Journal of Pharmaceutical Research October 2017; 16 (10): 2331-2339
ISSN: 1596-5996 (print); 1596-9827 (electronic)

Available online at http://www.tjpr.org
http://dx.doi.org/10.4314/tjpr.v16i10.4

Original Research Article

Synthesis, characterization and evaluation of biological activities of manganese-doped zinc oxide nanoparticles

Shakeel Ahmad Khan[1]*, Sammia Shahid[1], Waqas Bashir[1], Sadia Kanwal[2] and Ahsan Iqbal[3]

[1]Department of Chemistry, University of Management and Technology, Lahore-54000, [2]Department of Biochemistry, University of Agriculture, [3]Government College University Faisalabad-38000, Pakistan

For correspondence: **Email: Shakilahmad56@gmail.com; **Tel:** +92-3441865064*

Sent for review: 12 May 2017 *Revised accepted: 16 September 2017*

Abstract

Purpose: *To synthesize, characterize and investigate the antimicrobial properties of pure and manganese-doped zinc oxide nanoparticles.*
Method: *Un-doped and manganese-doped zinc oxide (Mn-doped ZnO) nanoparticles were prepared using co-precipitation method. The synthesized Mn-doped ZnO nanoparticles were characterized using energy-dispersive x-ray spectroscopy (EDX), scanning electron microscopy (SEM), and x-ray diffraction (XRD) spectroscopic techniques. Their band gap energies were measured with ultraviolet-visible (UV-Vis) spectroscopy, while their antioxidant properties were evaluated by ferric reducing antioxidant power (FRAP), DPPH radical-scavenging, ferric thiocyanate (FTC) and total phenolic content (TPC) assays. The antimicrobial activities of the nanoparticles against different bacterial strains were determined using agar diffusion method.*
Result: *Results from XRD, SEM, EDX and UV-Vis analyses demonstrated successful synthesis of un-doped and Mn-doped ZnO nanoparticles as seen in their hexagonal, wurtzite structures. The un-doped and Mn-doped ZnO nanoparticles had average grain sizes of 16.72 nm and 17.5 nm, and band gap energies of 3.585 eV and 2.737 eV, respectively. Significant antibacterial activity was manifested by Mn-doped ZnO against E. coli, S. aureus, Klebsiella and B. subtilis, with zones of inhibition (ZOIs) of 13 ± 0.09 mm, 14 ± 0.01 mm, 18 ± 0.07 mm and 20 ± 0.10 mm, respectively. The Mn-doped ZnO nanoparticles also exhibited effective and significant antioxidant potential relative to butylated hydroxytoluene (BHT) and un-doped ZnO nanoparticles.*
Conclusion: *Mn-doped ZnO nanoparticles demonstrate significant antimicrobial and antioxidant activities. Thus, the preparation is a good candidate for further development into therapeutic formulations.*

Keywords: *Mn-doped ZnO, Nanoparticles, Properties, Antioxidant, Antibacterial*

Tropical Journal of Pharmaceutical Research is indexed by Science Citation Index (SciSearch), Scopus, International Pharmaceutical Abstract, Chemical Abstracts, Embase, Index Copernicus, EBSCO, African Index Medicus, JournalSeek, Journal Citation Reports/Science Edition, Directory of Open Access Journals (DOAJ), African Journal Online, Bioline International, Open-J-Gate and Pharmacy Abstracts

INTRODUCTION

Zinc oxide (ZnO) nanoparticles have received much attention in recent years due to their diverse applications [1]. Nowadays, prototype ZnO nanoparticles are used as delivery systems for vaccines and anti-cancer drugs [2]; as antimicrobial agents, additives in industrial products and photo-catalysts for disintegrating organic materials [3]. However, ZnO nanostructures are still being widely studied with a view to enhancing their potential applications in the field of biomedicine [2].

It has been reported that the functionality and efficiency of ZnO nanoparticles and

nanostructures can be improved by increasing and modifying their surface areas through nano-scale addition of some dopants materials such as biomolecules and transition metals (Mn, Fe, Cr, Cu) [4]. This surface modification with biomolecules and transition metals confers new properties on ZnO nanoparticles so they can function as biosensors, antimicrobial, antioxidants, drug delivery systems and bio-imaging materials [1,4,5].

Different methods have been developed for the fabrication of un-doped ZnO and transition metal-doped ZnO nanoparticles [6]. Manganese (Mn) is the metal of choice for doping of ZnO nanoparticles because of the ready availability of its d electrons at t_2g level, and also for the fact that these electrons can easily overlap with the valance bond of ZnO nanoparticles [4,5].

It has been demonstrated that if ZnO nanoparticles are doped with Mn, the products have enhanced antibacterial [2] and magnetic properties [3] which may be acceptable for biomedical and spintronic applications [4]. The enhancement of the antioxidant and antimicrobial properties is due to the fact that doping of ZnO nanoparticles with Mn increases the surface area and reduces particle size of ZnO nanoparticles [7], Thus, studies aimed at investigating the biological, optical, and magnetic properties of Mn-doped ZnO nanoparticles have attracted much interest [8].

The purpose of the present study was to synthesize and characterize un-doped ZnO and Mn-doped ZnO nanoparticles, and investigate their antibacterial and antioxidant properties.

EXPERIMENTAL

All chemicals and reagents used were procured from Sigma-Aldrich (United States of America) and Merck (Germany) and were of analytical grade. These reagents included butylated hydroxytoluene (BHT; 99.07% pure); 2, 2-diphenyl-1-picrylhydrazyl (DPPH, 90.0% pure); Folin-Ciocalteu reagent (2N), linoleic acid and catechin.

Preparation of solutions

Zinc acetate [$Zn(CH_3COO)_2.2H_2O$; 0.05M)] was prepared by dissolving 5.525 g of Zn-acetate in distilled water in a 500-mL volumetric flask, with solution level brought up to the mark, and then stirring for 10 min. Thereafter, 0.05M solution of magnesium acetate [$Mn(CH_3COO)_2.4H_2O$] was prepared by dissolving 1.235 g of Mn-acetate in 100 mL distilled water in a measuring flask, followed by vortexing. Ammonia solution (35 %) was also prepared in distilled water.

Synthesis of un-doped ZnO nanoparticles

Zinc acetate (0.05 M, 450mL) was put in a 1000-mL beaker and stirred for 30 min at room temperature (30 ^oC) using magnetic stirrer at the rate of 2000 rpm. Diluted ammonia (35 %) was added slowly with constant stirring for 1 h, to a pH of about 10. After attaining the desired pH~ 10, the reaction mixture was heated at 60 ^oC with continuous stirring for 30 min using magnetic stirrer at the rate of 2000 rpm. Then reaction mixture was placed at room temperature (28-30 ^oC) for 48 h for precipitation to occur. This resulted in the formation of white colored precipitates in the reaction mixture. To separate the precipitates, the reaction mixture was filtered and washed thrice with distilled water, and then further washed thrice with 30 mL of ethanol to remove impurities. Thereafter, the precipitates were filtered and oven-dried at 110 ^oC for 1 h. The dried precipitates were milled using a pestle and mortar, and then the powder was heated in oven for 20 min at the same temperature (110 ^oC) to remove any absorbed moisture. Then, calcination of the white powder was done at 200 ^oC for 3 h in a muffle furnace. This yielded white and fine un-doped ZnO nanoparticles which were kept in air tight container at room temperature (25-30 ^oC).

Synthesis of Mn-doped ZnO nanoparticles

The zinc acetate and manganese acetate solutions were employed, and ammonia (35 %) was used to adjust the pH to 10. To 450 mL of 0.05M Zn acetate in a 1000-mL beaker was slowly and continuously added, with stirring, 50 mL of 0.05M Mn acetate. The reaction mixture was stirred for 30 min using magnetic stirrer at the rate of 2000 rpm. Diluted ammonia was then added from the burette to the reaction mixture, at a flow rate of 2 mL/min to attain pH~ 10. The reaction mixture was constantly stirred during the pH adjustment, at the rate 1000 rpm in a magnetic stirrer. After the pH adjustment, the solution was further stirred with the magnetic stirrer at the rate of 1500 rpm for 1 h. Then the reaction mixture was heated at 60 ^oC for 30 min, and placed at room temperature (28-30 ^oC) for 48 h for precipitation to take place. This resulted in the formation of brown-colored precipitates in the reaction mixture. To separate out the precipitates, the reaction mixture was filtered and washed thrice with distilled water, and then washed thrice with 30 mL of ethanol to eliminate impurities. The precipitates were thereafter oven-dried at 110 ^oC for 1 h, and milled in a pestle and

mortar. The brown, powdered nanoparticles were heated in an oven for 20 min at 110 ^{o}C to remove any traces of absorbed moisture. Then, calcination of the brown powder was done at 200 ^{o}C for 3 h in a muffle furnace. This yielded brown and fine Mn-doped ZnO nanoparticles that were kept in an air-tight container at room temperature (25-30 ^{o}C) prior to use [9].

Characterization of un-doped and Mn-doped ZnO nanoparticles

Energy dispersive X-ray technique was employed for the determination of the composition and morphology of the synthesized un-doped and Mn-doped ZnO nanoparticles. In addition, characterization of the crystalline structure of the nanoparticles was done using the XRD i.e. PANalytical X'Pert diffractometer instrument with Cu-Kα radiation (wavelength 0.154 nm) operating at 40 kV and 30 mA. Measurements were scanned for diffraction angles (2θ) ranging from 20 to 90^{o} with a step size of 0.02^{o} and a time per step of 1 s. The absorption spectrum and band gap energies of the synthesized nanoparticles were determined by UV-visible spectrophotometer (Spectra Flash SF 550, Data color Inc., USA), while their morphological features were determined using SEM (Jeol, 5910LV).

Evaluation of antioxidant activity

DPPH free radical scavenging assay

The antioxidant properties of the un-doped and Mn-doped ZnO nanoparticles were determined by 2, 2-diphenyl-1-picrylhydrazyl (DPPH) radical scavenging capacity according to the method of Khan *et al* [10]. Butylated hydroxytoluene (BHT) was used as standard for comparison.

Total phenolic content (TPC) assay

The total phenolic content of the Mnu-doped ZnO NAPs was determined colorimetrically as described by Khan *et al* [11].

Ferric reducing antioxidant power (FRAP) assay

Antioxidant potential of un-doped and Mn-doped ZnO nanoparticles was also assessed by evaluating the ferric reducing antioxidant power as described by Ijaz *et al* [12].

Ferric thiocyanate (FTC) assay

Antioxidant potential in terms of the inhibitory effect of the un-doped and Mn-doped ZnO nanoparticles on linoleic acid peroxidation was evaluated by the thiocyanate method of Ijaz *et al.* [12].

Evaluation of antibacterial activity

The antibacterial properties of the synthesized un-doped and Mn-doped ZnO nanoparticles were evaluated by using the Agar well diffusion method of Khan *et al* [13, 14]. The bacterial strains used for the determination of bactericidal activities were *Bacillus subtilis* (*B. subtitles*), *Escherichia coli* (*E. coli*), *Klebsiella* and *Staphylococcus aureus* (*S. aureus*). *S. aureus, Klebsiella and Bacillus subtilis* represented Gram-positive bacteria *while E. coli* represented Gram-negative bacteria. Distilled water was used as negative control for the bacterial strains while bacteriological cephradine was used as standard antibiotic for positive control. Solutions of un-doped ZnO and Mn-doped ZnO nanoparticles in distilled water were prepared through ultra-sonication method. Two different concentrations of solutions (3 and 5 mg/mL) for the synthesized un-doped ZnO and Mn-doped ZnO nanoparticles were used for evaluating the antibacterial potential, and the results were compared with those obtained for the standard drug (cephradine). For the reference antibiotic, 1 mg was used in the present study.

Statistical analysis

Statistical analysis was done by one-way or two-way ANOVA and the Tukey post-test using Graph Pad Prism v6.04 software (Graph Pad Software, Inc., La Jolla, CA, USA). Differences were considered statistically significant at $p<0.05$. Group sizes are indicated in the figure legends. All values are expressed as mean ± SD.

RESULTS

Characteristics of synthesized nanoparticles

X-ray diffraction

The XRD patterns for un-doped and Mn-doped ZnO nanoparticles are shown in Figure 1 (a) and Figure (b) respectively. The XRD pattern of un-doped ZnO nanoparticles was uniform and no impurities were observed in the spectrum as shown in Figure 1(a). Moreover, the XRD pattern showed intense and sharp peaks which confirmed the crystalline nature of the un-doped ZnO nanoparticles. The formation of phase indicates pure wurtzite structure of ZnO nanoparticles which was confirmed by XRD peaks 31.7, 34.35, and 36.15. As the highest

peak (36.15) is the major peak homologous to hexagonal wurtzite structure.

The XRD results indicate good crystalline nature of un-doped ZnO nanoparticles because of intense and narrow peaks. The average grain size of un-doped ZnO nanoparticles was 16.72 nm. Moreover, small broadening at the bottom of peaks indicated that the crystalline size was small [7]. The XRD pattern for Mn-doped ZnO nanoparticles is shown in Figure 1 (b). The XRD patterns of Mn-doped ZnO nanoparticles were similar to those of XRD pattern of un-doped ZnO nanoparticles. The XRD results demonstrated that the peaks were narrow and sharp which confirmed the crystalline nature of the synthesized Mn-doped ZnO nanoparticles.

The average grain size for Mn-doped ZnO nanoparticles was 17.5 nm. The average size was slightly greater than that of the un-doped ZnO nanoparticles, obviously due to incorporation of Mn. Grain size depends on percentage of doping element. The formation of phase indicated pure wurtzite structure of Mn-doped ZnO nanoparticles which was confirmed by XRD peaks 25.65, 29.80, 31.30, 33.95, and 35.75. Figure 2(b) shows uniform XRD pattern, with no evidence of impurity in the Mn-doped ZnO nanoparticles [8]. The grain sizes of the un-doped and Mn-doped ZnO nanoparticles were calculated by Debye-Scherer's formula.

Morphological characteristics

Figures 2 (a) and (b) show the surface morphological and structural patterns of un-doped ZnO nanoparticles using scanning electron microscope (SEM). SEM micrograph for un-doped ZnO nanoparticles indicated that the un-doped ZnO nanoparticles were fine particles with crystalline behavior. Moreover, SEM results also confirmed that the synthesized un-doped ZnO nanoparticles had particles size in nanometer in range.

Figure 2 (c) shows the micrograph for Mn-doped ZnO nanoparticles. SEM micrograph results demonstrated that the particle size of Mn-doped ZnO nanoparticles was slightly larger than that of

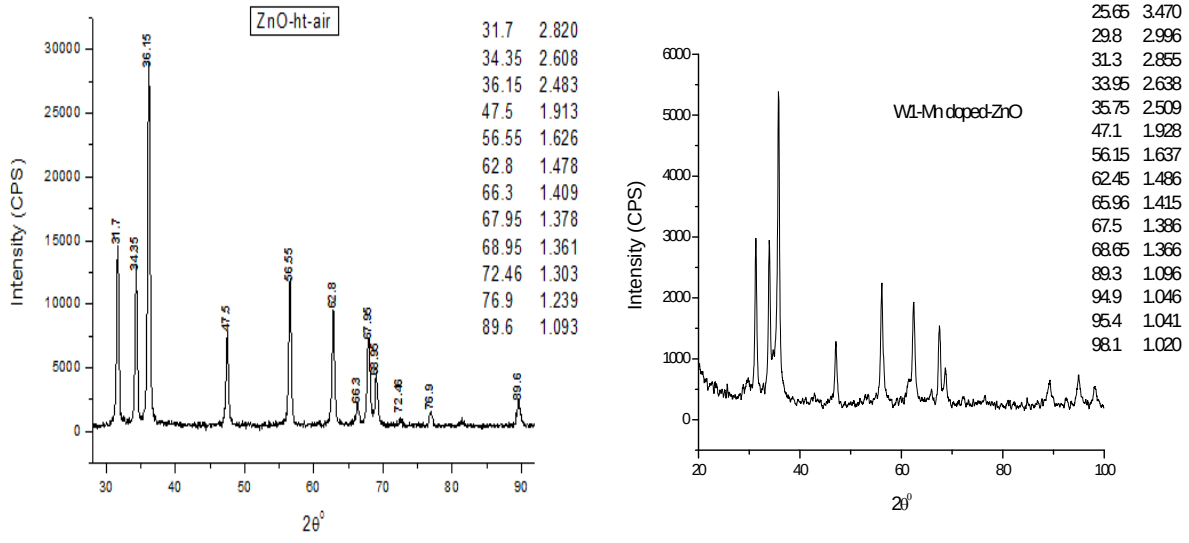

(a) **(b)**

Figure 1: XRD pattern of un-doped ZnO (a) and Mn-doped ZnO nanoparticles (b)

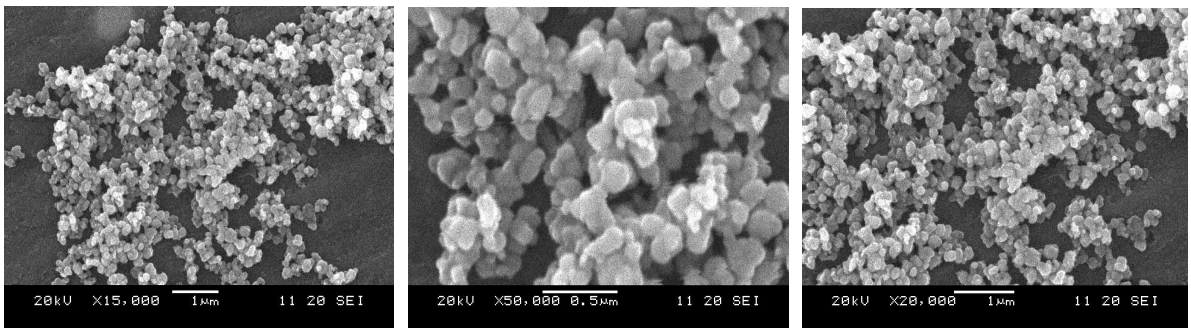

(a) **(b)** **(c)**

Figure 2: SEM micrographs of un-doped ZnO (a), (b) and Mn-doped ZnO nanoparticles (c)

the un-doped ZnO nanoparticles. The enlargement of the particles size is due to the doping with Mn. The same structural behavior of Mn-doped ZnO nanoparticles was observed in XRD results in terms of particles size. Moreover, Figure 2 also indicates that the synthesized nanoparticles had good crystalline nature. A close relationship was observed between the results of XRD and SEM. The SEM images showed seed-like structures of un-doped ZnO and Mn-doped ZnO nanoparticles which are consistent with earlier reports [15].

EDX analysis

EDX studies were carried out in order to examine the chemical formation and composition of the synthesized nanoparticles and also to confirm the presence of un-doped ZnO and Mn-doped ZnO nanoparticles. Figures 3 (a) and (b) show the EDX spectra for un-doped ZnO and Mn-doped ZnO nanoparticles, respectively. EDX spectra confirmed the presence of the constituents zinc (Zn), oxygen (O) in the nanoparticles. Hence, EDX spectra affirmed the presence of un-doped ZnO and Mn-doped ZnO nanoparticles in the synthesized sample. It was clear from the EDX pattern that the nanoparticles were successfully synthesized. The consistent and sharp peaks with zinc oxide and manganese-zinc oxide demonstrated that both synthesized nanoparticles were crystalline in nature, and that peaks associated with impurities were absent in EDX spectra of both nanoparticles (un-doped ZnO and Mn-doped ZnO) [9]. Hence, nanoparticles were obtained in their pure forms.

Band gap energy data

Band gap is referred to as energy difference between the top valence bands and the bottom conduction band. It reflects the ability of electron

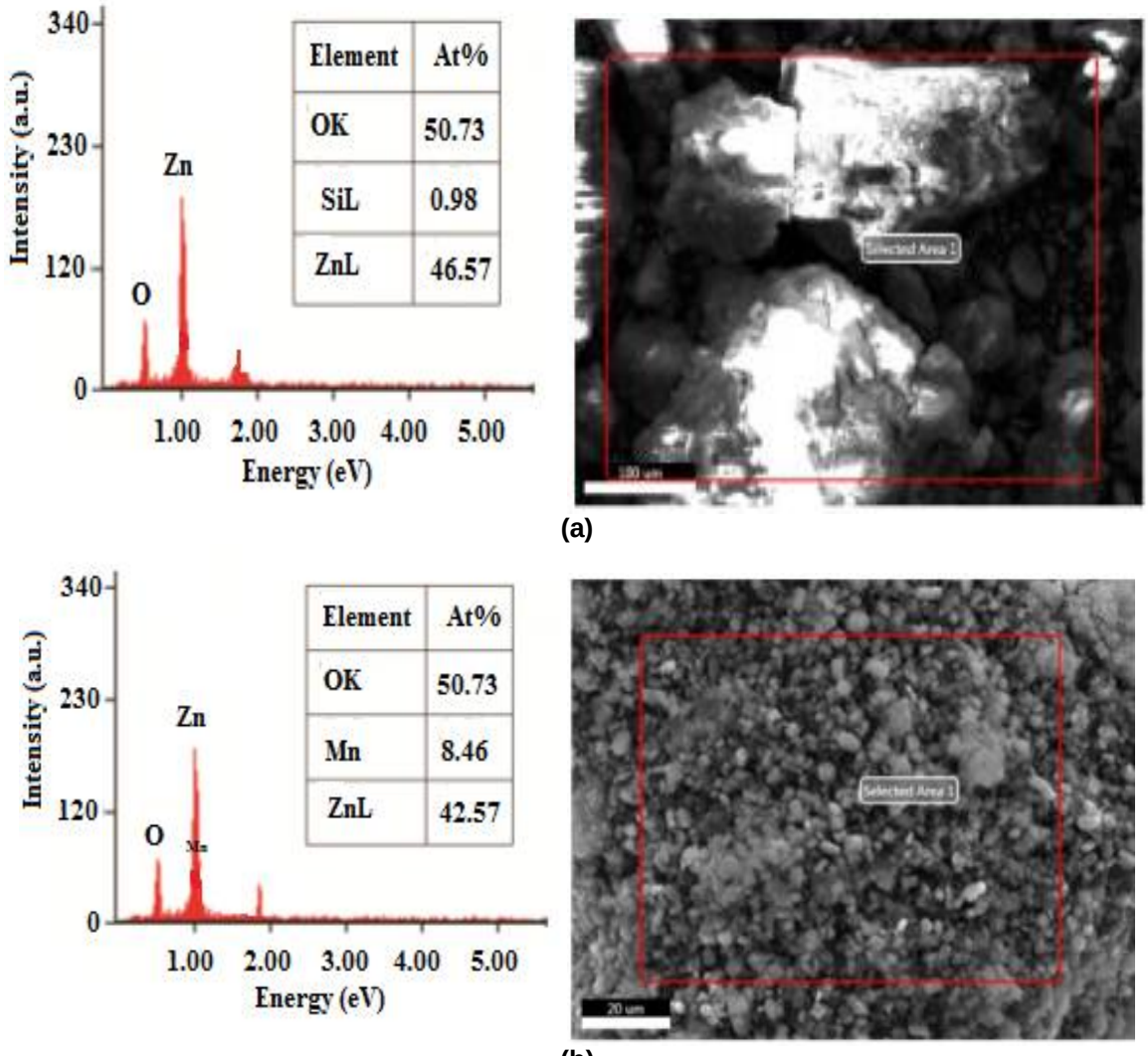

Figure 3: EDX spectrum of un-doped ZnO (a) and Mn-doped ZnO nanoparticles (b)

to jump from one band to another. A specific minimum amount of energy is required for this transition. Measurement of band gap plays a vital role in semiconductors. The band gap energy of an insulator is large (> 4 eV), but is lower for a semiconductor (< 3 eV) [16]. The value of E_g is achieved by the intersection between the photon energy axis and linear fit. The band gap energy of un-doped ZnO nanoparticles was 3.375 eV; while for Mn-doped ZnO nanoparticles, band gap energy of 2.737 eV was obtained [Figures 4 (a) and (b)]. Since t_{2g} level (i.e. the dxy, dxz, and dyz orbitals are collectively called the t2g orbitals) of Mn is very close to valence bonds (VB) of ZnO, the d-electrons of Mn can easily overlap with the valence band of ZnO [17]. Being semiconductors, the band gap energy of Mn-doped ZnO nanoparticles should be less than 3 eV. This is in agreement with the band gap energy value for Mn-doped ZnO nanoparticles in this study, which was less than 3 eV (Figure 4 b).

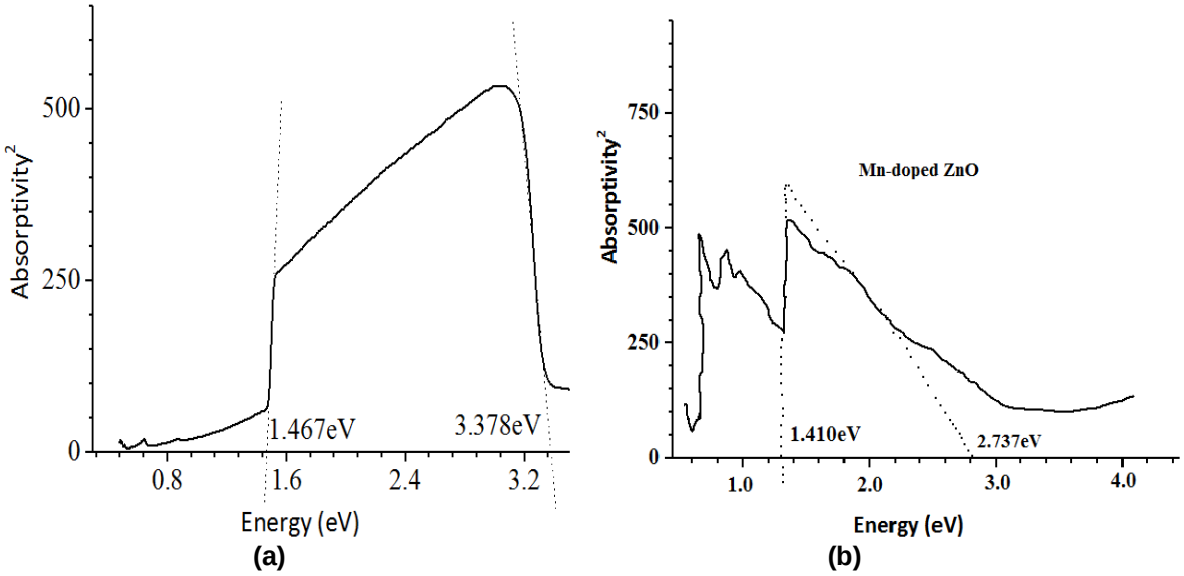

Figure 4: Band gap energy data of un-doped ZnO (a) and Mn-doped ZnO nanoparticles (b)

Antioxidant activity

The results of DPPH radical scavenging assay for different concentrations of un-doped ZnO nanoparticles are shown in Table 1 in the form of IC_{50} values. The lowest IC_{50} value (41 ± 0.32 µg/mL) was seen at a concentration of 1000 µg/mL, while the highest IC_{50} value (85 ± 0.23 µg/mL) was obtained at a concentration of 60 µg/mL for un-doped ZnO nanoparticles.

In the case of Mn-doped ZnO nanoparticles, the lowest IC_{50} of 39 ± 0.22 µg/mL was obtained at a concentration of 1000 µg/mL and the highest IC_{50} of 78 ± 0.25 µg/mL was seen at 60 µg/mL. The DPPH free radical scavenging activity increased with increasing concentration of the Mn-doped ZnO nanoparticles. At a level 1000 µg/mL, Mn-doped ZnO nanoparticles showed significant DPPH radical scavenging activity comparable to that of BHT with IC_{50} value of 48 ± 0.29 µg/mL. This indicates that the Mn-doped ZnO nanoparticles possess high antioxidant activities in terms of scavenging of DPPH free radicals.

High level of total phenolic content (20.1 ± 0.21 mg/100g GAE) was obtained at a concentration of 1000 µg/mL, while the lowest total phenolic content (0.95 ± 0.08 mg/100g GAE) was observed at 60 µg/mL of un-doped ZnO nanoparticles. A similar pattern was seen at different concentrations of Mn-doped ZnO nanoparticles, although the corresponding values were higher when compared with un-doped ZnO nanoparticles (the percentage of total phenolic contents varied from 1.09 ± 0.18 to 23.1 ± 0.31 mg/100g GAE at various concentrations i.e. 60 125, 250, 500 and 1000 µg/mL of Mn-doped ZnO nanoparticles). These results are shown in Table 1, and they indicate that the TPCs of the un-doped ZnO and Mn-doped ZnO nanoparticles were concentration-dependent. The results of antioxidant activities of different concentrations of un-doped and Mn-doped ZnO nanoparticles, with respect to inhibition of linoleic acid oxidation, are shown in Table 1. The percentage inhibition values of linoleic acid peroxidation were 18 ± 0.23, 31 ± 0.19, 43 ± 0.15, 50 ± 0.17 and 63 ± 0.21 at 60, 125, 250, 500 and 1000 µg/mL, respectively, for un-doped ZnO nanoparticles. Maximum percentage inhibition was 63 ± 0.21% (at 1000 µg/mL), while the minimum percentage inhibition (18 ± 0.23 %) was recorded at 60 µg/mL. For Mn-doped ZnO nanoparticles, percentage inhibitions varied from 21 ± 0.13 to

65 ± 0.11%. Higher inhibition of linoleic acid oxidation was observed in Mn-doped ZnO nanoparticles than in un-doped ZnO nanoparticles. Linoleic oxidation was significantly inhibited by the un-doped ZnO and Mn-doped ZnO nanoparticles at all the levels tested, and the percentage inhibition was comparable to that of BHT which produced 61 ± 0.19 % inhibition.

In the FRAP assay, maximum antioxidant activity of 8.99 ± 0.21 µM/mL TE was produced by 1000 µg/mL while minimum antioxidant activity of 0.59 ± 0.01 µM/mL TE was observed with 60 µg/mL of un-doped ZnO nanoparticles. The antioxidant activity of Mn-doped ZnO nanoparticles varied from 0.79±0.11 to 10.9 ± 0.11 µM/mL TE. Higher FRAP was exhibited by Mn-doped ZnO nanoparticles than un-doped ZnO nanoparticles. These results are also shown in Table 1.

Antibacterial activity

The results of antibacterial activity of the un-doped ZnO and Mn-doped ZnO nanoparticles are shown in Tables 2 and 3. The un-doped ZnO nanoparticles, at 5 mg and at 3 mg exhibited significant antibacterial activities against *B. subtilis,* with ZOIs of 17 ± 0.11 mm and 15 ± 0.07 mm, respectively. Against *Klebsiella,* the ZOIs were 15 ± 0.05 and 13 ± 0.04 mm, respectively. At 5 and 3 mg, the un-doped ZnO nanoparticles demonstrated effective bactericidal activity with minimum inhibitory concentrations (MICs) of 0.09 and 0.13 mg/mL, respectively for *Klebsiella*.

MICs of 0.07 and 0.04 mg/mL were obtained at 3 mg and at 5 mg, respectively for *B. subtilis*. Compared to the standard drug cephradine (1 mg), it was evident that 5 mg was much more effective for *Klebsiella* and *B. subtilis*.

ZOIs of cephradine for *Klebsiella* and *B. subtilis* were 12±0.05 mm and 14±0.09 mm, respectively. Higher bactericidal potential was exhibited by Mn-doped ZnO nanoparticles relative to the standard drug and un-doped ZnO nanoparticles (Table 3). Mn-doped ZnO nanoparticles (at 5 mg) produced stronger inhibition of the growth of *E. coli, S. aureus*, *Klebsiella* and *B. subtilis,* with ZOIs of 13 ± 0.09, 14 ± 0.01, 18 ± 0.07 and 20 ± 0.10, respectively. The MICs of Mn-doped ZnO nanoparticles (at 5 mg) ranged from 0.03 to 0.09 mg/mL. Thus, the Mn-doped ZnO nanoparticles showed very effective broad spectrum antibacterial activities.

Table 1: Antioxidant activity of synthesized un-doped ZnO and Mn-doped ZnO nanoparticles

S/no.	Concentration (µg/mL)	DPPH (IC_{50}, µg/mL)	FRAP (µM/mL as TE)	TPC (mg/100g as GAE)	Inhibition of linoleic acid oxidation (%)
M1 NAPs					
1	60	85±0.23	0.59±0.01	0.95±0.08	18±0.23
2	125	71±0.30	1.88±0.12	2.01±0.11	31±0.19
3	250	68±0.29	3.01±0.09	5.01±0.15	43±0.15
4	500	56±0.33	4.68±0.19	11.2±0.25	50±0.17
5	1000	41±0.32	8.99±0.21	20.1±0.21	63±0.21
6	BHT	48±0.29	-	-	61±0.19
M2 NAPs					
1	60	78±0.25	0.79±0.11	1.09±0.18	21±0.13
2	125	65±0.36	2.08±0.02	4.99±0.01	35±0.29
3	250	58±0.25	4.01±0.19	8.01±0.25	48±0.05
4	500	49±0.20	7.40±0.09	15.3±0.05	56±0.27
5	1000	39±0.22	10.9±0.11	23.1±0.31	65±0.11
6	BHT	48±0.29	-	-	61±0.19

Values are mean ± SD (n = 3); M1 NAPs = un-doped ZnO nanoparticles, M2 NAPs = Mn-doped ZnO nanoparticles

Table 2: ZOIs in antibacterial test of un-doped ZnO nanoparticles against different bacterial strains

Bacterial strain	Inhibition zone diameter (mm)			MIC (mm)		
	Standard (1 mg)	*M1 NAPs (5 mg)*	*M1 NAPs (3 mg)*	*Standard (1 mg)*	*M1 NAPs (5 mg)*	*M1 NAPs (3 mg)*
E. coli	11±0.09	8±0.08	7±0.04	0.30	0.80	0.95
S. aureus	13±0.05	11±0.11	8±0.09	0.10	0.95	1.01
Klebsiella	12±0.05	15±0.05	13±0.04	0. 14	0.09	0.13
B. subtilis	14±0.09	17±0.11	15±0.07	0.08	0.04	0.07

Values are mean ± SD (n = 3). M1 NAPs = un-doped ZnO nanoparticles, MIC= Minimum inhibition concentration, Standard = cephradine

Table 3: ZOIs in antibacterial test of Mn-doped ZnO nanoparticles against different bacterial strains

Bacterial strain	Inhibition zone diameter (mm)			MIC (mm)		
	Standard (1mg)	***M2 NAPs (5mg)***	***M2 NAPs (3mg)***	***Standard (1mg)***	***M2 NAPs (5mg)***	***M2 NAPs (3mg)***
E. coli	11±0.09	13±0.09	9±0.05	0.30	0.09	0.90
S. aureus	13±0.07	14±0.01	11±0.08	0.10	0.08	0.85
Klebsiella	12±0.05	18±0.07	14±0.05	0.14	0.07	0.11
B. subtilis	14±0.09	20±0.10	17±0.06	0.08	0.03	0.05

Values are mean ± SD (n =). M2 NAPs = Mn-doped ZnO nanoparticles, MIC= Minimum inhibition concentration, Standard = ephradine

DISCUSSION

XRD spectra demonstrated that the presence of intense and sharp peaks in the XRD spectra of the synthesized un-doped ZnO and Mn-doped ZnO nanoparticles. This confirmed their crystalline nature. The average calculated grain size of the un-doped ZnO and Mn-doped ZnO nanoparticles were 16.72 and 17.5 nm, respectively. These results demonstrate that the grain size of the doped ZnO nanoparticles is larger than that of the un-doped ZnO nanoparticles. This is due to the fact that Mn doping results in an increase in grain size. Thus the grain size of ZnO nanoparticles was increased by Mn doping. The particle size was decreased due to increase in the percentage of Mn or doping with Mn. These findings are in agreement with previous reports [18,19].

SEM results affirmed the nanoscale range of particle size for the un-doped ZnO and the Mn-doped ZnO nanoparticles and also confirmed their wurtzite crystalline structures [15]. Results from EDX were consistent with those from SEM and XRD. The major constituents of the nanoparticles were Zn, O and Mn. The strong, intense, narrow width and sharp peaks in the EDX spectrum indicated that the un-doped ZnO and Mn-doped ZnO were crystalline in nature [15]. There were agreement and close relationship in the results of the various characterization techniques, which is an indication of successful synthesis of the nanoparticles. Band gap data was lower in Mn-doped ZnO nanoparticles than in the un-doped ZnO. This is likely due to the fact that Mn doping decreased band gap energy value since the band gap energy obtained for the doped product was less than 3.0 eV value for semiconductors [16,17].

Different concentrations of the synthesized un-doped ZnO and Mn-doped ZnO were investigated for antioxidant potential through total antioxidant assays (DPPH radical scavenging, FRAP, inhibition of linoleic acid peroxidation and TPC). Mn-doped ZnO nanoparticles produced better antioxidant results than the un-doped ZnO nanoparticles and BHT, while un-doped ZnO nanoparticles showed antioxidant activity comparable to BHT. This was due to the fact that doping with Mn enhanced the antioxidant activity of un-doped ZnO nanoparticles [5]. The results also revealed that the antioxidant activities of the nanoparticles were concentration-dependent [12]. These results are consistent with previously reported data [8,20,21].

The un-doped ZnO nanoparticles at 5mg produced higher antibacterial effects than the standard drug cephradine in the inhibition of growth of *Klebsiella*, and *Bacillus subtilis,* while the Mn-doped ZnO nanoparticles exhibited greater bactericidal effect in contrast to standard drug and un-doped ZnO nanoparticles in inhibiting the growth of these organisms. This significant bactericidal activity was due to the release of Mn^{+2} ions and Zn^{+2} from Mn-doped ZnO nanoparticles, and the permeation of the bacterial cell membrane by these ions. The permeation of Mn^{+2} and Zn^{+2} ions was possible due to the attraction of their positive charges to the negatively-charged cell wall. The binding of these ions destroyed the bacterial cell membrane. In addition, Mn^{+2} ions and Zn^{+2} ions are involved in cross-linkage of nucleic acid strands by binding with DNA molecules of bacteria. This produces a disorder in the DNA structure, leading to protein denaturation and complete destruction of the bacterial cell [5,20,21].

CONCLUSION

The results of this study indicate that although the synthesized un-doped ZnO nanoparticles possess potent and desirable biological properties such as antibacterial and antioxidant activities, Mn-doped ZnO nanoparticles showed better results than un-doped ZnO nanoparticles. This is due to the large surface and smaller particle size of Mn-doped nanoparticles. Thus, the synthesized nanoparticles hold enormous potential for use in the cosmetic, nutraceutical and pharmaceutical industries.

DECLARATIONS

Acknowledgement

This work was supported by the Department of Chemistry, School of Science, University of Management and Technology, Lahore, Pakistan.

Conflict of Interest

No conflict of interest associated with this work.

Contribution of Authors

The authors declare that this work was done by the authors named in this article and all liabilities pertaining to claims relating to the content of this article will be borne by them.

REFERENCES

1. *Anukaliani A, Manjula G, Nair M, Nirmala M, Rekha K. Structural, optical, photocatalytic and antibacterial activity of ZnO and Co doped ZnO nanoparticles. Mat Lette 2011; 65: 1797-1800.*
2. *Gubin SP. Magnetic nanoparticles. Wiley-VCH 2009; ISBN 3-527-40790-1.*
3. *Yadav A, Parsad V, Kathe AA, Raj S, Yadav D, Sundaramoorthy C, Vigneshwaran N. Functional finishing in cotton fabrics using zinc oxide nanoparticles. Bull Mater Sci 2006; 29: 641-645.*
4. *Djuisic AB, Leung YH, Choy WCH, Cheah KW, Chan WK. Visible photoluminescence in ZnO tetrapod and multipod structure. Appl Phys Lett 2004; 84(14): 2635-2637.*
5. *Reddy KM, Feris K, Bell J, Wingett DG, Hamley C, Punnoose A. Selective toxicity of zinc oxide nanoparticles to prokaryotic and eukaryotic system. Appl Phys Lett 2007; 90: 2139021-2139023.*
6. *Yan XX, Xu GY. Effect of sintering atmosphere on the electrical and optical properties of (ZnO)1-x(MnO2)x NTCR Ceramics. Physica B 2009; 404(16): 2377-2381.*
7. *Abdollahi Y, Abdullah H, Zainal Z, Yusof NA. Synthesis and characterization of Mn-doped ZnO nanoparticles. Int J Bas appl Sci 2011; 11(04): 62-69.*
8. *Wang Y, Zhao X, Duan L, Wand F, Niu H, Guo W, Ali A. Structure luminescence and photocatalytic activity of Mn-doped ZnO nanoparticles prepared by auto combustion method. Mat Sci Semi Process 2015; 29: 372-379.*
9. *Chawla S, Jayanthi SK. Fabrication of ZnO:Mn nanoparticles with organic shell in a highly alkaline aqueous environment. Appl Surf Sci 2011; 257: 2935-2939.*
10. *Khan SA, Rasool N, Riaz M, Nadeem R, Rashid U, Rizwan K, Zubair M, Bukhari IH, Gulzar T. Evaluation of Antioxidant and Cytotoxicity Studies of Clerodendrum inerme. Asian J Chem 2013; 13: 7457-7462*
11. *Khan SA, Shahid S, Jameel M, Ahmad A. In vitro antibacterial, antifungal and GC-MS analysis of seeds of Mustard Brown. Int J Pharm Chem 2016; 6(4): 107-115.*
12. *Ijaz F, Shahid S, Khan SA, Ahmad W, Zaman S. Green synthesis of copper oxide nanoparticles using Abutilon indicum leaf extract: Antimicrobial, antioxidant and photocatalytic dye degradation activities. Trop J Pharm Res 2017; 16(4): 743-753.*
13. *Khan SA, Shahid S, Khan ZA, Iqbal A. Assessment of stabilization of canola oil, free radical scavenging and cytotoxic potential of Peucedanum graveolens (roots). Int J Sci and Res Pub 2016; 6(3): 529-535.*
14. *Khan SA, Shahid S, Ahmad W, Ullah S. Pharmacological Importance of Clerodendrum Genus: A Current Review. Int J Pharm Sci Res 2017; 2(2): 22-30.*
15. *Tam KH, Djurisic AB, Chan CMN, Xi YY, Tse CW, Leung YH, Chan WK, Leung FCC, Au DWT. Antibacterial activity of ZnO nanoroads prepared by a hydrothermal method. Thi Sol Film 2008; 516(18): 6167-6174.*
16. *Hoffman M, Martin S, Choi W, Behnemann D, Environmental applications of semiconductor photo catalysis. Chem Rev 1995; 95: 69-96.*
17. *Halperin B, Lax M. Impurity-band tails in the high-density limit I. Minimum counting methods. Phys Rev 1966; 148(2): 722-740.*
18. *Yang M, Guo ZX, Qui K, Long J, Yin G, Guan D, Liu S, Zhou S. Synthesis and characterization of Mn-doped ZnO column arrays. Appl Surf Sci 2010; 256(13): 4201-4205.*
19. *Straumal B, Baretzky B, Mazilkin A, Protasava S. Increase of Mn solubility with decreasing grain size in ZnO. J Eur Cera Soci 2009; 29: 1963-1970.*
20. *Ahmad W, Khan SA, Munawar KS, Khalid A, Kanwal S. Synthesis, characterization and pharmacological evaluation of mixed ligand-metal complexes containing omeprazole and 8-hydroxyquinoline. Trop J Pharm Res 2017; 16(5): 1137-1146.*
21. *Khan SA, Shahid S, Sajid MR, Noreen F, Kanwal S. Biogenic Synthesis of CuO Nanoparticles and their Biomedical Applications: A Current Review. Int J Adv Res 2017; 5(6): 925-946.*